Regular Article

blood

THROMBOSIS AND HEMOSTASIS

Impaired von Willebrand factor adhesion and platelet response in thrombospondin-2 knockout mice

Nina Kristofik,[1] Nicole E. Calabro,[2] Weiming Tian,[2] Aaron Meng,[1] Susan MacLauchlan,[2] Yinong Wang,[2,3] Christopher K. Breuer,[4] George Tellides,[3] Laura E. Niklason,[1,5] and Themis R. Kyriakides[1,2]

[1]Department of Biomedical Engineering, School of Engineering and Applied Science, [2]Department of Pathology, and [3]Department of Surgery, School of Medicine, Yale University, New Haven, CT; [4]Department of Surgery, Nationwide Children's Hospital, Columbus, OH; and [5]Department of Anesthesiology, School of Medicine, Yale University, New Haven, CT

Key Points

- Irregular ECM assembly in TSP2 KO mice results in reduced VWF adhesion and compromised platelet function.
- Because overall ECM composition is not altered, this study highlights the importance of ECM organization in hemostasis and thrombosis.

Interactions between collagenous extracellular matrices and von Willebrand factor (VWF) are critical for hemostasis and thrombosis. In the present study, we investigated the contribution of an extracellular matrix (ECM) abnormality to the bleeding diathesis in thrombospondin-2 (TSP2) knockout (KO) mice. First, we performed adoptive bone marrow transplantation and observed that introduction of wild-type (WT) marrow into lethally irradiated TSP2 KO mice did not rescue the bleeding diathesis. However, platelets in transplanted mice displayed an inherent aggregation defect, which complicated interpretation. Second, we performed interposition of arterial segments denuded of endothelium. Denuded TSP2 KO arteries grafted into WT mice remained patent in vivo. In contrast, WT grafts underwent thrombosis and were completely occluded within 24 to 48 hours. The nonthrombogenic property of the TSP2 KO ECM was confirmed in vitro by exposing platelets to TSP2 KO dermal fibroblast (DF)-derived ECM. To further probe the effect of TSP2 deficiency, ECM production and deposition by WT and TSP2 KO DFs was analyzed via polymerase chain reaction, immunofluorescence, and scanning electron microscopy and showed similar patterns. In addition, atomic force microscopy (AFM) analysis of WT and TSP2 KO ECM did not reveal differences in stiffness. In contrast, reduced VWF accumulation on TSP2 KO ECM was observed when matrices were subjected to plasma under physiological flow. AFM utilizing VWF-coated 2-μm beads confirmed the weak binding to TSP2 KO ECM, providing a mechanistic explanation for the lack of thrombus formation. Therefore, our studies show that ECM assembly is critical for interaction of collagen with VWF and subsequent thrombogenic responses. (*Blood*. 2016;128(12):1642-1650)

Introduction

The extracellular matrix (ECM) forms the basis of the microenvironment within which cells exist in vivo, and, as such, it influences their behavior. The use of cell-derived ECM as a bioactive substrate for modulation of cell function has become an area of interest for many researchers. For example, the pioneering studies of Gospodarowicz et al showed a permissive effect of decellularized ECM on cell proliferation.[1] In addition, Vogel's group demonstrated altered matrix production by fibroblasts cultured on fibroblast-derived ECM.[2] In the same study, it was shown that cross-linking the substrate ECM postdecellularization led to its accelerated stretching by seeded cells. Thus, in addition to composition, cross-linking of decellularized ECM can modulate cell function. Of particular interest was that endothelial cell (EC)-derived ECM thrombogenicity was reduced by glutaraldehyde fixation or heat denaturation.[3] Consistent with this observation, cross-linking of decellularized vein also resulted in decreased thrombogenicity.[4]

Obvious considerations in determining the nature of cell-ECM interactions are the ECM's assembly and composition following decellularization. Presently, little is known about how ECM assembly occurs, even for well-studied proteins such as laminin.[5] Moreover, a more in-depth consideration of collagen fibrillogenesis is hindered by the fact that the process can occur in a cell-free environment. However, in the presence of cells, the initiation of fibrillogenesis requires noncollagenous molecules. Thus, the role of cells in a process driven by self-assembly and polymerization remains unclear. One hypothesis suggests the involvement of molecules such as collagens V and XI to nucleate collagen fibrils and fibronectin (FN) and integrins to specify their site of assembly.[6] This suggestion is supported by our knowledge of FN fibril assembly and its requirement for collagen fibril assembly. In addition, it has been shown that newly assembled collagen and FN fibrils colocalize.[7] Moreover, another class of noncollagenous molecules including N-propeptides of collagen, lysyl oxidase, tenascin-X, several proteoglycans, and thrombospondin-2 (TSP2) influences the rate of assembly, size, and structure of collagen fibrils.

TSP2 is an antiangiogenic, matricellular protein that has been shown to interact not only with ECM proteins, but also with a variety of

Submitted March 2, 2016; accepted July 1, 2016. Prepublished online as *Blood* First Edition paper, July 28, 2016; DOI 10.1182/blood-2016-03-702845.

The online version of this article contains a data supplement.

There is an Inside *Blood* Commentary on this article in this issue.

The publication costs of this article were defrayed in part by page charge payment. Therefore, and solely to indicate this fact, this article is hereby marked "advertisement" in accordance with 18 USC section 1734.

cell surface receptors.[8] Most of our current understanding of TSP2 function has been deduced from the investigation of TSP2 knockout (KO) mice and their cells. The TSP2 KO phenotype is dominated by abnormalities in connective tissue, which manifest as irregular collagen fibrillogenesis.[8] This aspect of the phenotype is also apparent in ECM derived in vitro from dermal fibroblasts (DFs) isolated from TSP2 KO mice.[9] Furthermore, TSP2 KO DF-derived ECM was more permissive for EC migration.[9] Our observations implicate the matrix-modulating activity of TSP2 as a novel mechanism in the regulation of ECM assembly. We have also previously reported that TSP2 KO mice display a bleeding diathesis that is due, in part, to a platelet aggregation defect.[10] Although the origin of the bleeding abnormality was reported to be the irregular interactions of megakaryocytes with the vascular sinuses in the TSP2 KO bone marrow microenvironment, we had not examined whether ECM assembly might contribute as well.[10]

In the current work, we have focused on platelet response to TSP2 KO ECM. As a follow-up to previous studies, we performed bone marrow transplants and found that wild-type (WT) marrow did not rescue the bleeding diathesis in TSP2 KO mice. However, analysis of TSP2 expression revealed none in megakaryocytes of transplanted mice. Moreover, platelets from these mice displayed an aggregation defect consistent with the TSP2 KO phenotype. Therefore, these experiments could not determine the contribution of an ECM defect to the bleeding phenotype. Further in vivo studies, in which aortas denuded of endothelium from TSP2 KO or WT mice were implanted into WT mice, showed that grafts from WT mice were occluded within 48 hours, whereas TSP2 KO grafts displayed no thrombosis, suggesting the presence of an ECM defect. This work prompted studies to determine potential mechanisms for the nonthrombogenicity of TSP2 KO ECM and to examine whether this property was retained in vitro. To probe for a mechanistic explanation, we examined ECM expression and deposition, mechanical properties, and adhesion of von Willebrand factor (VWF) to the ECM. Studies with platelets showed that TSP2 KO ECM had reduced thrombogenicity compared with that derived from WT cells. Our results showed that TSP2 KO ECM is unable to support the binding of VWF. Moreover, it is intriguing to consider the potential of TSP2 KO ECM as an antithrombotic coating for blood-contacting devices and vascular grafts.

Materials and methods

Animals

TSP2 KO and littermate WT (C57BL6/129SVJ) mice aged 3 to 4 months were used. All animal studies were performed as procedures approved by the institutional animal care and use committees of Yale University.

Bone marrow transplant

WT and TSP2 KO mice were lethally irradiated (800 cGy) and rescued 24 hours later with single-cell suspensions of 5×10^6 donor bone marrow cells in prewarmed Hanks balanced salt solution via tail vein injection (n = 5 per group). Recipient animals were studied 4 weeks posttransplantation.

Bleeding time

Bleeding time was measured as described previously.[8]

Arterial denudation

Carotid arteries in mice that received bone marrow transplants were denuded of endothelium using a nylon thread as described previously.[10] After 10 minutes, carotid arteries were perfusion-fixed, harvested, washed with phosphate-buffered saline (PBS), and prepared for scanning electron microscopy (SEM).

To further examine the antithrombotic potential of the TSP2 KO matrix, 2-mm sections of abdominal aorta from WT and TSP2 KO 8- to 12-week mice were denuded of endothelium with nylon thread and interposed into the abdominal aortas of WT mice using an end-to-end anastomotic surgical technique as described previously.[11] After 48 hours (or earlier if in extremis), mice were anesthetized, perfused, and abdominal aortas were procured and fixed for histology.

Image analysis

Thrombus area and percent area covered by platelets were determined by analysis with ImageJ.

Preparation of TSP2 KO ECM

DFs from WT and TSP2 KO mice were isolated, plated into 24-well plates, and decellularized as described previously.[9]

Platelet and VWF studies

Platelet-rich plasma (PRP) or platelet-poor plasma (PPP) were isolated and prepared as described previously.[10] Platelet adhesion on WT, TSP2 KO, and TSP2 KO ECM treated overnight with 5 μg/mL TSP2 (R&D Systems) was examined by pipetting PRP onto decellularized matrix. Matrix and plasma were allowed to interact for 30 minutes with shaking at 37°C. WT and TSP2 KO PPP were used to determine VWF levels via an enzyme-linked immunosorbent assay (ThermoFisher). Adenosine 5′-diphosphate (ADP) aggregation experiments were performed as described previously.[10]

Flow chamber studies

WT and TSP2 KO matrices were produced on flow chamber glass slides. To prepare matrices, glass slides were placed in 1 M NaOH for 1 hour, rinsed (deionized water), and air-dried. Slides were autoclaved and coated with 1% gelatin before seeding with 250 000 cells. Cells were cultured and matrix was prepared as described in "Preparation of TSP2 KO ECM."

Matrix-coated slides were placed in a flow chamber as described previously.[12] Human plasma was flowed over slides for 15 minutes at 15 dynes/cm^2. After stopping flow, slides were collected, washed (PBS), and fixed (4% paraformaldehyde [PFA]).

Histology, immunohistochemistry, and electron microscopy

Tissue samples. All tissue samples collected and fixed (4% PFA) for histology were paraffin-embedded, sectioned, and mounted on glass slides. For initial visualization, tissues were stained with standard hematoxylin and eosin. Immunolocalization of TSP2 and PECAM-1 was performed as described previously.[8,9] Immunolocalization of VWF was performed after similar dewaxing and rehydration steps, but sections were incubated with fluorescein isothiocyanate–conjugated VWF antibody (Abcam) and 4′,6-diamidino-2-phenylindole (Invitrogen) for 30 minutes before mounting for fluorescent microscopy. Images were taken using Zeiss Axiovert 200 microscopes equipped with digital cameras.

All tissue samples collected for SEM during this study were fixed with 2% PFA in 0.1 M cacodylate buffer. After fixing, samples were dehydrated through an ethanol gradient and placed in hexamethyldisilazane. Samples were air-dried, sputter-coated with chromium, and viewed via SEM (Hitachi SU-70).

In vitro studies. Immunofluorescent examination of ECM proteins was performed on decellularized WT and TSP2 KO ECM. After decellularization, ECM was fixed (4% PFA), washed (PBS), and blocked (1% bovine serum albumin [BSA] in PBS) for 30 minutes. ECM was then incubated with antibodies to either collagen I, collagen III, collagen IV, collagen VI, FN, laminin (Abcam), TSP2 (BD Biosciences), or decorin (R&D Systems) overnight at 4°C. After washing (PBS), and incubation with secondary antibody (Invitrogen), samples were mounted for fluorescent microscopy.

Reverse transcriptase–polymerase chain reaction (RT-PCR) was performed on WT and TSP2 KO cells grown in ECM-producing conditions for 10 days before lysing in radioimmunoprecipitation assay buffer. RNA was isolated from cells (RNeasy; Qiagen) and reverse transcribed (QuantiTect Reverse

Table 1. Primer sequences used for Q-PCR of ECM proteins

ECM component	Forward	Reverse
Collagen I	TGACTGGAAGAGCGGAGAGTACT	CCTTGATGGCGTCCAGGTT
Collagen III	CTGTAACATGGAAACTGGGGAAA	CCATAGCTGAACTGAAAACCACC
Collagen IV	AACAACGTCTGCAACTTCGC	CTTCACAAACCGCACACCTG
Collagen V	CTTCGCCGCTACTCCTGTTC	CCCTGAGGGCAAATTGTGAAAA
Collagen VI	CTGCTGCTACAAGCCTGCT	CCCCATAAGGTTTCAGCCTCA
FN	GAGAGGAGCACTACCCCAGA	GCCCGGATTAAGGTTGGTGA
Decorin	AATGTGGGTGTCAGCTGGAT	CTAGCAAGGTTGTGTCGGGT

Q-PCR, quantitative PCR.

Transcription kit; Qiagen). PCR amplification was performed using primers for collagens I, III, IV, V, VI, FN, or decorin. Amplification of RPLP0 (ribosomal protein, large, P0) served as a control. See Table 1 for primer sequences.

Platelet adhesion was examined by fluorescence. Nonadherent platelets were removed (PBS wash); samples were fixed and stained with rhodamine-phalloidin (Molecular Probes) according to standard procedures.

For flow studies, immunolocalization was performed on fixed slides. To confirm matrix retention under flow conditions, slides were stained for FN as described at the beginning of this section. In order to examine the interaction of VWF with decellularized matrices, some slides were incubated with fluorescein isothiocyanate–conjugated VWF antibody (Abcam) before washing (PBS) and mounting for fluorescent microscopy (Zeiss Axiovert 200).

Atomic force microscopy

Sample preparation. ECM samples were prepared as described in "Preparation of TSP2 KO ECM" on 8-well chamber slides (Nunc). Similarly, slides were coated with TSP1, TSP2 (R&D Systems), or collagen type I (BD Biosciences) by incubating 10 μg/mL purified protein in PBS at 4°C overnight. Samples to be analyzed by atomic force microscopy (AFM) were also treated with 1% BSA in PBS to prevent nonspecific binding to tissue-culture plastic. Slides coated with pure protein were stained via immunofluorescence after AFM to ensure protein coverage and retention.

Cantilever preparation. Carboxylated polystyrene beads 2 μm in diameter (Invitrogen) were attached to tipless cantilevers (Bruker) with UV-curing adhesive using a micromanipulator. Recombinant VWF (Millipore) was subsequently conjugated via 1-ethyl-3-(3-dimethylamino) propyl carbodiimide/N-hydroxysuccinimide chemistry to the beads on cantilevers. Bead attachment and VWF conjugation were confirmed via light and fluorescent microscopy, respectively (supplemental Figure 1, available on the *Blood* Web site).

Force measurements. A Bruker Dimension Icon AFM, equipped with a camera for live viewing of the ECM, was used to determine modulus and adhesion force. All measurements were performed using a fluid tip holder in 0.2× PBS. Cantilever calibration was performed before each set of measurements by analyzing force curves generated by cantilevers on a standard fused silica sample (Bruker) using the Nanoscope Analysis software to calculate deflection sensitivity. The thermal tune function of the Dimension AFM software was then used to calculate the cantilever's spring constant. For each sample, 15 to 20 force curves were collected at 2 to 3 areas selected for force measurements using a ramp rate of 0.5 Hz and a trigger threshold equivalent to the application of 2 nN of force. Force curves were analyzed for Young Modulus (n = 8) and adhesion force (n = 5) using Nanoscope Analysis software.

Statistical analysis

All data presented are expressed as means ± standard error of the mean. Statistical differences were determined by either Student *t* tests or 1-way analysis of variance. A value of $P < .05$ was considered to be significant.

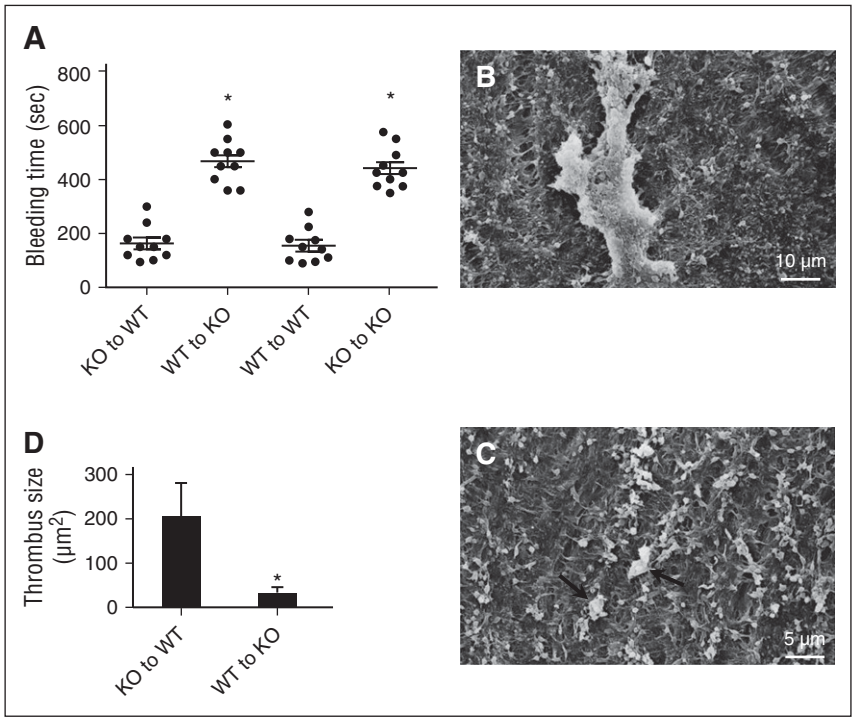

Figure 1. Vessel ECM abnormality contributes to the bleeding diathesis in TSP2 KO mice. (A) Rescue of irradiated WT and KO mice with KO and WT bone marrow cells, respectively, did not alter the bleeding time of the host. In addition, homotypic rescue maintained the original phenotype. Transplant of WT bone marrow to irradiated TSP2 KO mice did not reduce the bleeding time. Circles (●) denote individual mice. (B-C) Representative SEM images of denuded carotid arteries from WT mice receiving TSP2 KO bone marrow (B) and TSP2 KO mice receiving WT bone marrow (C) 10 minutes after wire injury. (D) Quantification of thrombus size by ImageJ revealed a decrease in TSP2 KO arteries. *$P < .05$

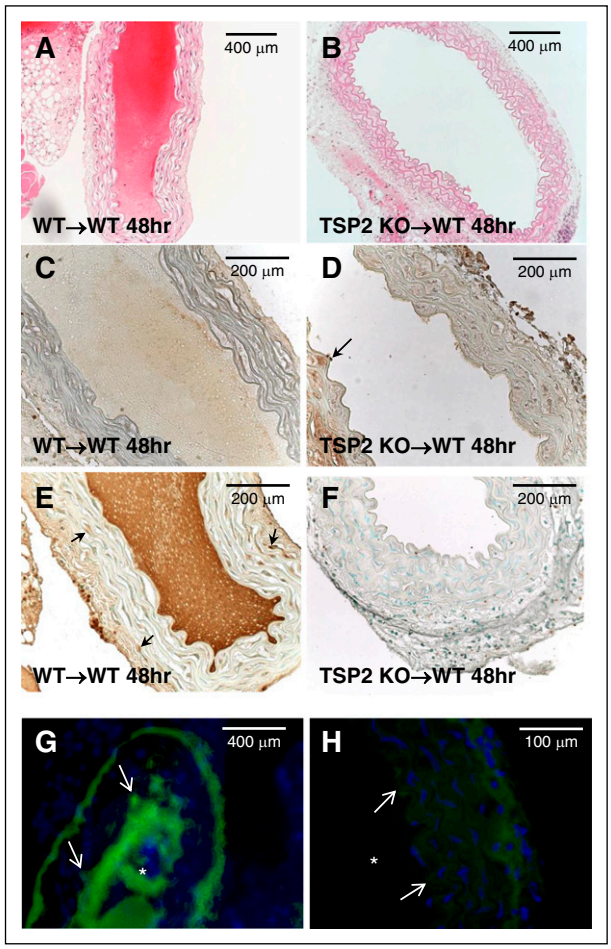

Figure 2. TSP2-null denuded aortic grafts resist thrombosis. Aortic segments from WT and TSP2 KO mice were denuded and grafted in WT mice. Representative images of hematoxylin-and-eosin (H&E)-stained sections of grafts 48 hours following surgery are shown. WT to WT graft (A) is completely occluded whereas the KO to WT graft is fully patent (B) (Zeiss). (C-D) Representative images of WT (C) and TSP2 KO (D) aortic segments immunostained for PECAM-1 (brown color) are shown and demonstrate lack of endothelium. Arrow in D denotes remnants of endothelium. (E-F) Representative images of WT (E) and TSP2 KO (F) aortic segments immunostained for TSP2 (brown color) are shown and demonstrate presence and absence of TSP2, respectively. Arrows in E denote TSP2-immunoreactive cells. (G-H) Representative images of immunofluorescence detection of VWF (green color) in WT (G) and TSP2 KO (H) aortic segments are shown (Zeiss). WT segments show excessive VWF immunoreactivity in the area of thrombus formation, which is absent in TSP2 KO grafts. Asterisk (*) denotes lumen area; arrows denote the vessel edge. Sections were counterstained with methyl green (A-F) or DAPI (G-H). n = 5.

Results

Adoptive bone marrow transplantation and platelet function

We previously reported a bleeding diathesis in TSP2 KO mice and that platelets from TSP2 KO mice displayed suboptimal ADP-induced aggregation in vitro.[10] In order to probe these defects, adoptive bone marrow transfers were performed. Both WT and TSP2 KO mice were lethally irradiated and rescued with bone marrow from either WT or TSP2 KO donors. Successful transplantation was confirmed by detection of the WT and KO allele in KO and WT mice, respectively (data not shown). Because TSP2 is not expressed in circulating cells and cannot be detected in blood, we analyzed bone marrow by immunohistochemistry. Previously, it was shown that marrow stromal cells produce TSP2.[13] One month after transplantation, TSP2-positive megakaryocytes were detected in WT recipients rescued with either WT or TSP2 KO bone marrow suggesting that irradiation-resistant MSCs remain a source for the protein (supplemental Figure 2). In contrast, we were unable to detect TSP2 in bone marrow of TSP2 KO recipients regardless of donor genotype. In addition, analysis of platelet response to ADP revealed normal aggregation in PRP from WT mice rescued with either genotype, and suboptimal aggregation in PRP from TSP2 KO mice rescued with either genotype (supplemental Figure 2). We also determined platelet numbers and found no differences among any of the groups (WT→KO, 730 000 ± 85 498; KO→WT, 601 000 ± 68 636; WT→WT, 698 000 ± 53 609; KO→KO, 726 000 ± 75 208), nor were they different from previously reported platelet counts of WT and TSP2 KO mice.[8] To exclude the possibility that VWF levels could differ between WT and TSP2 KO mice, we performed a VWF enzyme-linked immunosorbent assay and found no differences (27.97 ± 0.45 ng/mL for WT and 28.61 ± 0.61 ng/mL for TSP2 KO; n = 3). Bleeding times were determined and it was found that WT mice receiving WT and TSP2 KO bone marrow had bleeding times that did not differ from each other, nor from those of previously reported untransplanted WT mice (132 seconds).[8] In contrast, TSP2 KO mice receiving WT and TSP2 KO bone marrow had longer bleeding times, comparable to those of untransplanted TSP2 KO mice (552 seconds) (Figure 1A).[8]

In order to probe this defect further, we denuded the endothelium of the carotid arteries in bone marrow transplanted TSP2 KO to WT and WT to TSP2 KO mice. Thrombus formation was greater in WT mice rescued with TSP2 KO marrow (Figure 1B) vs TSP2 KO mice rescued with WT marrow (Figure 1C). Image analysis confirmed significantly increased thrombus area in bone marrow transplanted WT mice (Figure 1D). These observations are consistent with a role for TSP2 in megakaryocyte function and production of normal platelets.

Denuded TSP2 KO arteries do not cause thrombosis

Although the previous experiments indicate a platelet defect in all TSP2 KO mice, they do not exclude the contribution of a matrix abnormality to the bleeding diathesis. In order to probe this possibility while circumnavigating the platelet variable, segments of aortas from either WT or TSP2 KO donor animals were removed, denuded of endothelium, and grafted into the abdominal aortas of WT mice. WT to WT grafts were all occluded and resulted in the death of all animals within 48 hours (n = 5) (Figure 2A). WT recipients receiving TSP2 KO grafts, however, were all alive and the grafts showed no signs of thrombus at 48 hours (n = 5) (Figure 2B). PECAM-1 staining confirmed endothelial denudation of grafts (Figure 2C-D). TSP2 staining demonstrated that TSP2 KO grafts did not contain TSP2, whereas TSP2 was present in WT grafts (Figure 2, panels F and E, respectively). Immunofluorescence for VWF showed almost no VWF bound to TSP2 KO ECM in comparison with significant VWF bound to WT ECM and in the thrombi (Figure 2, panels H and G, respectively). Because all graft recipients were WT animals, platelets and VWF levels were not variables in these experiments. Therefore, the results suggest that TSP2 KO ECM does not support normal platelet aggregation and this defect, in addition to platelet abnormalities, could play a significant role in their bleeding phenotype.

WT and TSP2 KO ECM are expressed and deposited in similar quantities and patterns, and ECM mechanical properties are unchanged

ECM expression and deposition by TSP2 KO and WT DFs was then examined. Previously, we reported that collagen fibrils in TSP2 KO ECM are irregular in shape compared with collagen fibrils in WT ECM in vitro.[9,14] In an attempt to identify differences in individual

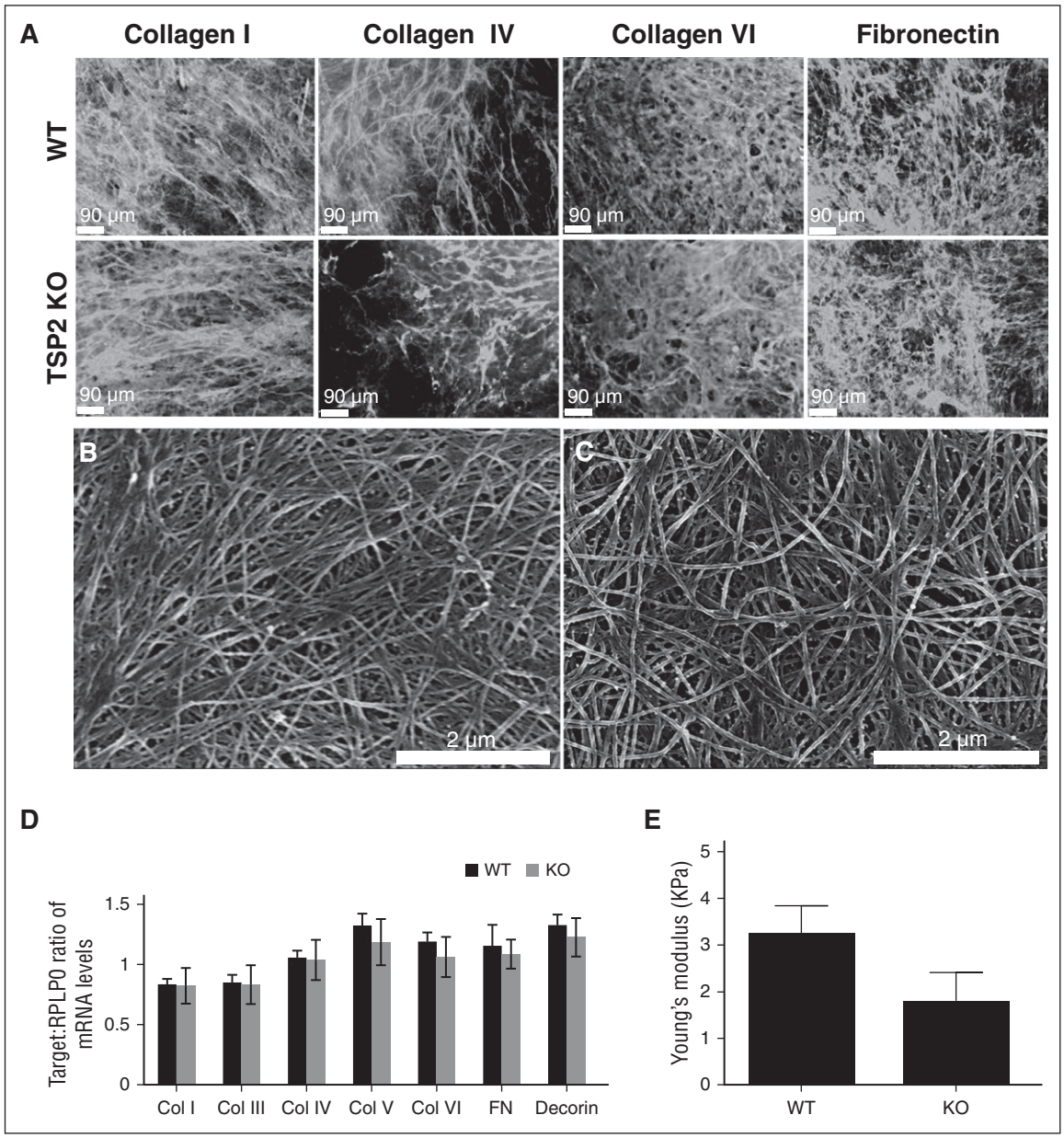

Figure 3. Analysis of protein expression, deposition, and ECM mechanical properties. (A) Representative images of immunofluorescence detection of several ECM components in DF-derived decellularized WT and TSP2 KO ECM (Zeiss). (B-C) Representative SEM images of WT (B) and TSP2 KO (C) decellularized ECM deposited on tissue-culture plastic. Collagen fibril arrangement appeared less aligned in the latter (Hitachi). (D) PCR analysis of several ECM proteins expressed by WT and TSP2 KO DFs revealed similar levels of expression. (E) Determination of ECM Young Modulus by AFM. A 2-μm bead affixed to the end of an AFM cantilever was used to perform nanoindentation studies on WT and TSP2 KO ECM. After force curves were collected, Young Modulus was determined using NanoScope Analysis software. n = 8. Col, collagen.

components of WT and KO ECM, we performed immunofluorescence for collagens I, IV, and VI, and FN (Figure 3A), as well as for collagen III, laminin, and decorin (supplemental Figure 3). Immunofluorescence showed similar deposition patterns in WT and TSP2 KO ECM for all components analyzed. Moreover, SEM imaging of WT and TSP2 KO ECM did not reveal striking differences, though WT collagen fibrils were more aligned than those of TSP2 KO matrix (Figure 3, panels B and C, respectively). RT-PCR showed no difference in messenger RNA content for collagens I, III, IV, V, VI, FN, or decorin between WT and TSP2 KO cells (Figure 3D).

It is known that skin from TSP2 KO mice is less stiff than comparable tissue from WT animals, as measured by tensile testing.[8] However, until recently it has been difficult to confirm whether this property is retained in cell-derived matrix. AFM is a method for measuring the mechanical properties of thin and delicate materials, such as hydrogels and cell-derived ECM.[15,16] Therefore, we determined the stiffness of WT and TSP2 KO ECM using this method. Although we found a trend toward decreased stiffness of TSP2 KO ECM compared with WT ECM, the difference was not significant (n = 8) (Figure 3E).

Reduced thrombogenicity of TSP2 KO ECM

To determine whether the nonthrombotic phenotype was retained in vitro, we prepared decellularized ECM from WT and TSP2 KO DFs and evaluated the ability of each to support platelet aggregation. Fluorescence showed significant aggregation of platelets on WT ECM (Figure 4A). In contrast, platelet adhesion was sparse with no aggregate formation on TSP2 KO ECM (Figure 4B). Costaining for FN verified

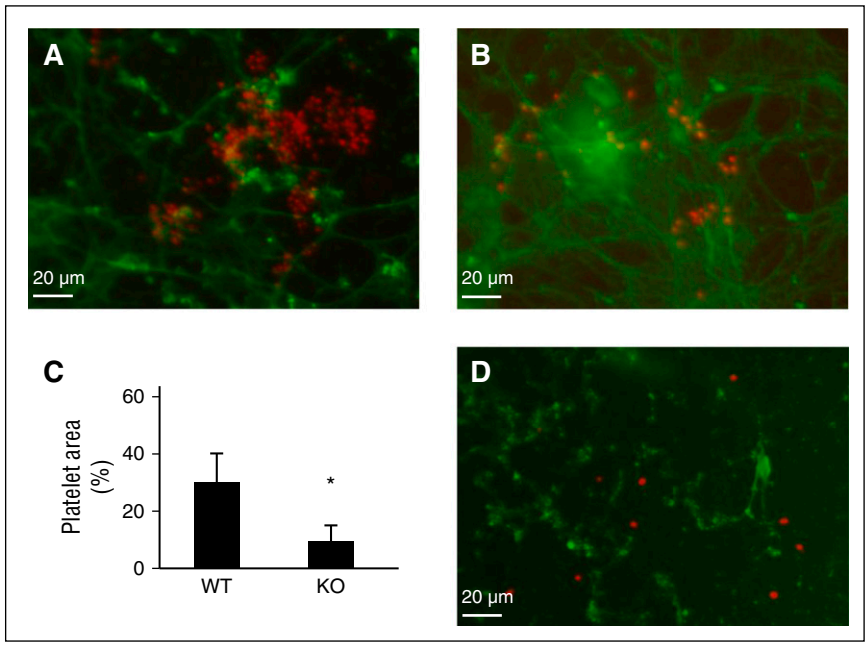

Figure 4. Cell-derived TSP2 KO ECM does not support platelet aggregation. DF-derived ECM was prepared in vitro following decellularization of long-term (7 days) cultures. Mouse platelets were exposed to either WT or TSP2 ECM for 30 minutes. (A-C) Representative images of platelets visualized by rhodamine-phalloidin (red color) on WT (A) or TSP2 KO ECM are shown. Detection of FN (green color) confirms the retention of ECM during the duration of the experiment (Zeiss). (C) Quantification of platelet area by ImageJ showed reduced platelet aggregation on TSP2 KO ECM. n = 5; $^*P < .05$. (D) Incubation of TSP2 KO ECM with 5 μg/mL TSP2 (detected via immunofluorescence, green color) overnight did not appear to increase platelet aggregation on TSP2 KO ECM.

ECM retention and that platelet adhesion was specific to ECM. Image analysis indicated a decreased percentage of the image occupied by platelets on TSP2 KO ECM (Figure 4C). These results showed that platelets aggregate on WT ECM but to a lesser degree on TSP2 KO ECM produced in vitro. We have previously shown that TSP2 is retained in decellularized WT ECM.[14] To examine whether it

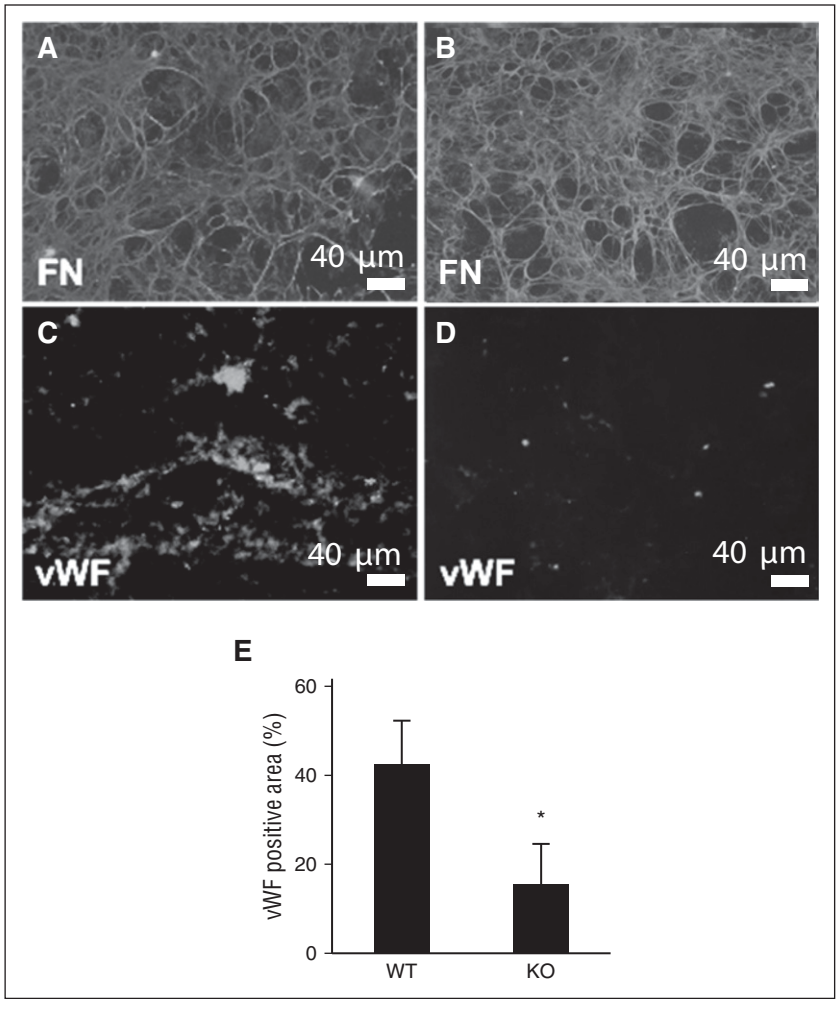

Figure 5. Reduced interaction of VWF with TSP2 KO derived ECM. DFs from WT (A, C) and TSP2 KO mice (B, D) mice were cultured for 10 days and then removed by decellularization. ECMs were then exposed to plasma under flow (15 dynes/cm^2) for 15 minutes. (A-B) Immunofluorescence detection of FN (green color) revealed retention of the ECM at the conclusion of the experiment. (C-D) VWF accumulation on ECM was detected by immunofluorescence (green color) (Zeiss). Interaction with TSP2 KO ECM (D) was minimal in comparison with WT (C) and this was confirmed by image analysis using ImageJ (E). n = 3; $^*P < .05$

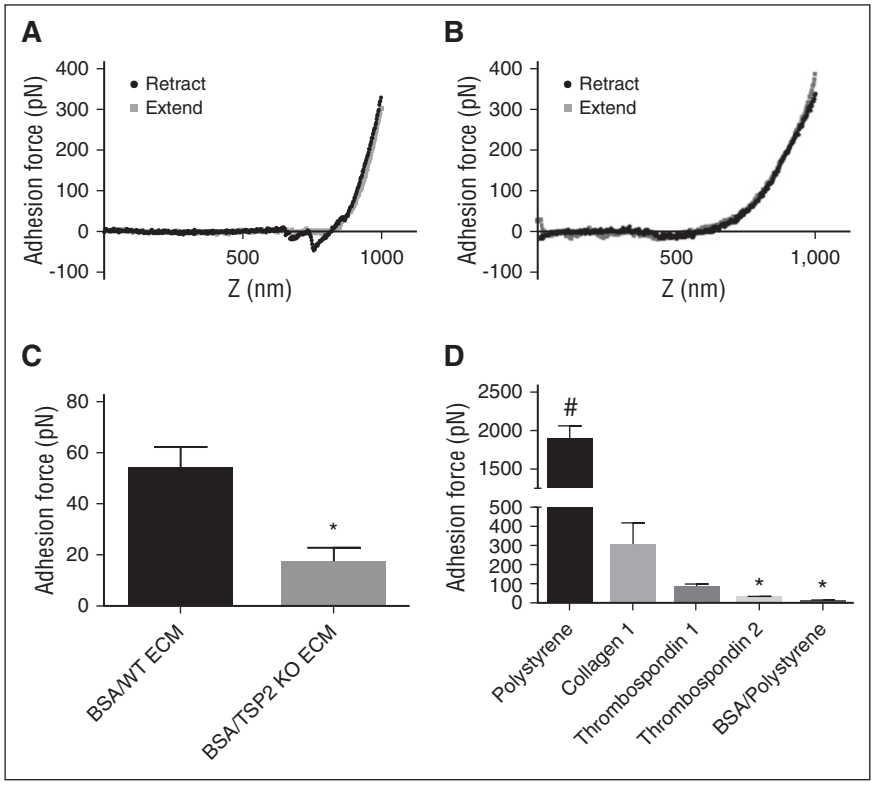

Figure 6. Reduced VWF adhesion force on TSP2 KO derived ECM as measured by AFM. A VWF-conjugated 2-μm bead affixed to the end of an AFM cantilever was used to perform adhesion force studies. These studies were performed on decellularized day 7 ECM from WT and TSP2 KO DFs after BSA treatment, as well as on untreated plastic, collagen, TSP1, and TSP2-coated plastic, and BSA-treated tissue-culture plastic controls. Representative AFM approach and retract curves for adhesion of VWF-coated bead to WT ECM (A), where there is significant adhesion (denoted by the downward spike in the retract curve) and TSP2 KO ECM (B), where there is no visible adhesion. Quantification of the adhesion force was performed using NanoScope Analysis software and showed reduced VWF adhesion on the TSP2 KO ECM compared with WT ECM (C) and no adhesion of VWF to pure TSP2 compared with collagen I and TSP1 (D). n = 5; $^*P < .05$; $\#P < .0001$.

contributes to platelet adhesion, TSP2 KO ECM was treated overnight with 5 μg/mL TSP2 and then exposed to platelets. Despite detection of TSP2 on the KO ECM, platelet aggregation was not evident indicating that it does not directly influence this process (Figure 4D).

VWF binding to TSP2 KO matrix is deficient

VWF plays a critical role in thrombus formation, as it is capable of binding to both exposed collagen and platelets. We examined binding of VWF to WT and TSP2 KO ECM using a system in which either WT or TSP2 KO ECM was deposited on glass slides, placed in a flow chamber, and exposed to human plasma at physiological flow rates (15 dynes/cm^2). After exposure to plasma under flow for 15 minutes, WT and TSP2 KO ECM were examined via immunofluorescence for FN, to ensure ECM had not been dislodged (Figure 5A-B), and for VWF (Figure 5C-D). Immunofluorescence detection of VWF showed decreased plasma-derived VWF binding to TSP2 KO ECM compared with WT ECM (Figure 5E).

AFM analysis shows distinct VWF adhesion forces

As mentioned in "WT and TSP2 KO ECM are expressed and deposited in similar quantities and patterns, and ECM mechanical properties are unchanged," TSP2 KO ECM showed a trend toward reduced stiffness in comparison with WT. However, the difference was not significant, suggesting that it cannot completely explain the lack of platelet response. To explore this defect further, we used an AFM approach capable of determining precise adhesion force measurements via a configuration involving a bead coated with VWF. Similar AFM techniques have previously been used to measure adhesive forces involved in platelet adhesion, such as glycoprotein Ib–VWF adhesion and integrin $\alpha_2\beta_1$–collagen peptide adhesion.[17,18] Based upon the decreased VWF staining on TSP2 KO ECM in vitro and in vivo, we investigated the adhesion force of VWF binding to cell-derived ECM. AFM studies in which VWF was conjugated to beaded cantilevers showed adhesion of VWF to WT ECM. This was measured by calculating the difference in force between the nadir of the adhesion spike (the depression into negative values of force) in the retract curve and the corresponding values of the approach curve (Figure 6A). Strikingly, no adhesion spike was seen in force curves from TSP2 KO ECM samples (Figure 6B). Adhesion forces were quantified and VWF adhesion was decreased on TSP2 KO ECM (16.47 ± 13 pN) compared with WT ECM (53.84 ± 18 pN) (Figure 6C). In addition, examination of VWF adhesion to purified proteins indicated adhesion to collagen I and TSP1 (positive controls), but not TSP2 (Figure 6D).

Discussion

The formation of ECM in association with cells is a complex process that is poorly understood. In order to gain a better understanding of the role of molecules modulating the nucleation and cellular assembly of ECM, many researchers have endeavored to alter their expression. Studies on collagen V, a molecule thought to be important in nucleation of collagen I fibrils, have shown that genetic ablation of the α1 component of collagen V leads to mechanical failure of skin at lower stresses. They have also shown that deletion of either the α1 or α2 components of collagen V results in larger, more irregularly shaped collagen fibrils.[19,20] Similar studies on lumican and decorin, which have been shown to increase interfibrillar spacing in acellular models, also yielded more delicate skin and connective tissue, as well as larger, irregular collagen fibrils.[21-24] In fact, it has been proposed that decorin-associated glycosaminoglycans act not only in fibril assembly, but also as bridges capable of transferring forces between fibrils.[25] So, it is possible that these kinds of molecules are not only important in the assembly of regular fibrils, but may also bolster the mechanical integrity of the mature fibers.

Large, abnormal collagen fibers and decreased mechanical strength of skin are also prominent aspects of the TSP2 KO mouse phenotype, though we have made repeated attempts to localize TSP2 in collagen fibers without success.[8,26] Our inability to demonstrate TSP2 as an integral component of collagen fibrils suggested that the abnormality in TSP2 KO mice could be due to a defect in collagen assembly by DFs.

In the current study, we examined the interactions of platelets with TSP2 KO ECM. Our interest in these interactions began when a bleeding diathesis was noted in TSP2 KO mice, though it was originally posited that this was due to a platelet defect.[10] However, as we have reported here, ECM assembled by DFs lacking TSP2 does not support aggregation of normal platelets. In healthy vessels, the ECM serves as a scaffold for the ECs, smooth muscle cells, and fibroblasts, with the ECs forming a barrier between the ECM and the blood. When the vessel is damaged, interactions between collagenous ECM and VWF have been shown to be critical for hemostasis and thrombosis. Once VWF is bound to collagen, it may in turn be bound by the platelet glycoprotein Ibα, tethering the platelet to the disruption in the endothelium. This is the first step toward thrombosis.[27] Simply by being accessible, ECM sets a crucial chain of events in motion. The fact that the TSP2 KO matrix does not seem to initiate this cascade is unusual. In order to elucidate a mechanism for this finding, we examined the expression and deposition patterns of components of WT and TSP2 KO ECM. In addition, we used AFM to examine the stiffness of and ability of DF-derived TSP2 KO ECM to support VWF adhesion. Notably, this information offers a potential mechanistic explanation for the reported platelet adhesion defect, as recent studies have shown that fibrin and collagen immobilized on stiffer substrates are more likely to activate platelets.[28,29] The inherent stiffness of TSP2 KO ECM was somewhat reduced and could partially contribute to compromised platelet responses. Analysis of adhesion strength of a 2-μm bead coated with VWF showed decreased adhesion force to TSP2 KO ECM, which was consistent with plasma flow studies showing reduced VWF accumulation on TSP2 KO ECM. We have also shown that VWF does not adhere to pure TSP2, which is consistent with the literature.[30] Taken together, these data and the fact that plasma VWF levels do not differ between WT and TSP2 KO mice indicate that the lack of VWF adhesion is associated with an ECM defect. We have previously shown that collagen fibril assembly by TSP2 KO DFs is irregular, and that cryptic collagen epitopes are exposed in TSP2 KO ECM.[9] As such, we are presently exploring the hypothesis that the VWF-binding defect is due to the effect of TSP2 deficiency on the formation of collagen fibrils. This fibril irregularity in turn could obscure VWF-binding sites, thus preventing the first step in the adhesion of platelets to the matrix. Further investigation will be required to confirm this hypothesis. Regardless of the mechanism, the antithrombotic nature of the TSP2 KO matrix coupled with the fact that it allows enhanced migration of endothelial cells,[9] suggests TSP2 KO ECM as a potential coating for devices and vascular grafts.

Acknowledgments

The authors thank Marcus Parrish and Jillian Andrejecsk for technical assistance and Priyanka Hardikar, Michael Rooks, and members of the Elimelech Laboratory for assistance with the AFM.

This work was supported by National Institutes of Health National Heart, Lung, and Blood Institute grants HL083895 (L.E.N.), HL107205 (T.R.K.), and HL098228 (C.K.B.), the National Science Foundation grant MRSEC DMR 1119826 (CRISP), and an American Heart Association predoctoral fellowship (N.K.).

Authorship

Contribution: N.K. designed the research, performed the experiments, analyzed the data, and wrote the paper; C.K.B., G.T., L.E.N., and T.R.K. designed the research and wrote the paper; and N.E.C., W.T., A.M., S.M., and Y.W. performed experiments and analyzed the data.

Conflict-of-interest disclosure: L.E.N. is a founder and shareholder in Humacyte, Inc, which is a regenerative medicine company. Humacyte produces engineered blood vessels from allogeneic smooth muscle cells for vascular surgery. L.E.N.'s spouse has equity in Humacyte, and L.E.N. serves on Humacyte's Board of Directors. L.E.N. is an inventor on patents that are licensed to Humacyte and that produce royalties for L.E.N. L.E.N. has received an unrestricted research gift to support research in her laboratory at Yale. Humacyte did not fund these studies, and Humacyte did not influence the conduct, description, or interpretation of the findings in this report. The remaining authors declare no competing financial interests.

The current affiliation for W.T. is Bio-X Center, School of Life Science and Technology, Harbin Institute of Technology, Harbin 150080, People's Republic of China.

Correspondence: Themis R. Kyriakides, Yale University, 10 Amistad St, Room 301C, New Haven, CT 06519; e-mail: themis.kyriakides@yale.edu.

References

1. Gospodarowicz D, Delgado D, Vlodavsky I. Permissive effect of the extracellular matrix on cell proliferation in vitro. *Proc Natl Acad Sci USA.* 1980;77(7):4094-4098.
2. Kubow KE, Klotzsch E, Smith ML, Gourdon D, Little WC, Vogel V. Crosslinking of cell-derived 3D scaffolds up-regulates the stretching and unfolding of new extracellular matrix assembled by reseeded cells. *Integr Biol (Camb).* 2009;1(11-12):635-648.
3. Vlodavsky I, Eldor A, HyAm E, Atzom R, Fuks Z. Platelet interaction with the extracellular matrix produced by cultured endothelial cells: a model to study the thrombogenicity of isolated subendothelial basal lamina. *Thromb Res.* 1982; 28(2):179-191.
4. Zhai W, Zhang H, Wu C, et al. Crosslinking of saphenous vein ECM by procyanidins for small diameter blood vessel replacement. *J Biomed Mater Res B Appl Biomater.* 2014;102(6): 1190-1198.
5. Hamill KJ, Kligys K, Hopkinson SB, Jones JC. Laminin deposition in the extracellular matrix: a complex picture emerges. *J Cell Sci.* 2009; 122(Pt 24):4409-4417.
6. Kadler KE, Hill A, Canty-Laird EG. Collagen fibrillogenesis: fibronectin, integrins, and minor collagens as organizers and nucleators. *Curr Opin Cell Biol.* 2008;20(5):495-501.
7. Li S, Van Den Diepstraten C, D'Souza SJ, Chan BM, Pickering JG. Vascular smooth muscle cells orchestrate the assembly of type I collagen via alpha2beta1 integrin, RhoA, and fibronectin polymerization. *Am J Pathol.* 2003;163(3): 1045-1056.
8. Kyriakides TR, Zhu YH, Smith LT, et al. Mice that lack thrombospondin 2 display connective tissue abnormalities that are associated with disordered collagen fibrillogenesis, an increased vascular density, and a bleeding diathesis. *J Cell Biol.* 1998;140(2):419-430.
9. Krady MM, Zeng J, Yu J, et al. Thrombospondin-2 modulates extracellular matrix remodeling during physiological angiogenesis. *Am J Pathol.* 2008; 173(3):879-891.
10. Kyriakides TR, Rojnuckarin P, Reidy MA, et al. Megakaryocytes require thrombospondin-2 for normal platelet formation and function. *Blood.* 2003;101(10):3915-3923.
11. Yu L, Qin L, Zhang H, et al. AIP1 prevents graft arteriosclerosis by inhibiting interferon-γ-dependent smooth muscle cell proliferation

and intimal expansion. *Circ Res.* 2011;109(4):418-427.

12. Yoo PS, Mulkeen AL, Dardik A, Cha CH. A novel in vitro model of lymphatic metastasis from colorectal cancer. *J Surg Res.* 2007;143(1):94-98.
13. Hankenson KD, Bornstein P. The secreted protein thrombospondin 2 is an autocrine inhibitor of marrow stromal cell proliferation. *J Bone Miner Res.* 2002;17(3):415-425.
14. Morris AH, Kyriakides TR. Matricellular proteins and biomaterials. *Matrix Biol.* 2014;37:183-191.
15. Soucy PA, Werbin J, Heinz W, Hoh JH, Romer LH. Microelastic properties of lung cell-derived extracellular matrix. *Acta Biomater.* 2011;7(1):96-105.
16. Zhu Y, Dong Z, Wejinya UC, Jin S, Ye K. Determination of mechanical properties of soft tissue scaffolds by atomic force microscopy nanoindentation. *J Biomech.* 2011;44(13):2356-2361.
17. Tobimatsu H, Nishibuchi Y, Sudo R, Goto S, Tanishita K. Adhesive forces between A1 domain of von Willebrand factor and N-terminus domain of glycoprotein Ibα measured by atomic force microscopy. *J Atheroscler Thromb.* 2015;22(10):1091-1099.
18. Attwood SJ, Simpson AM, Hamaia SW, et al. Measurement of the interaction between recombinant I-domain from integrin alpha 2 beta 1 and a triple helical collagen peptide with the GFOGER binding motif using molecular force spectroscopy. *Int J Mol Sci.* 2013;14(2):2832-2845.
19. Andrikopoulos K, Liu X, Keene DR, Jaenisch R, Ramirez F. Targeted mutation in the col5a2 gene reveals a regulatory role for type V collagen during matrix assembly. *Nat Genet.* 1995;9(1):31-36.
20. Sun M, Chen S, Adams SM, et al. Collagen V is a dominant regulator of collagen fibrillogenesis: dysfunctional regulation of structure and function in a corneal-stroma-specific Col5a1-null mouse model. *J Cell Sci.* 2011;124(Pt 23):4096-4105.
21. Stamov DR, Müller A, Wegrowski Y, Brezillon S, Franz CM. Quantitative analysis of type I collagen fibril regulation by lumican and decorin using AFM. *J Struct Biol.* 2013;183(3):394-403.
22. Chakravarti S, Magnuson T, Lass JH, Jepsen KJ, LaMantia C, Carroll H. Lumican regulates collagen fibril assembly: skin fragility and corneal opacity in the absence of lumican. *J Cell Biol.* 1998;141(5):1277-1286.
23. Danielson KG, Baribault H, Holmes DF, Graham H, Kadler KE, Iozzo RV. Targeted disruption of decorin leads to abnormal collagen fibril morphology and skin fragility. *J Cell Biol.* 1997;136(3):729-743.
24. Dourte LM, Pathmanathan L, Jawad AF, et al. Influence of decorin on the mechanical, compositional, and structural properties of the mouse patellar tendon. *J Biomech Eng.* 2012;134(3):031005.
25. Redaelli A, Vesentini S, Soncini M, Vena P, Mantero S, Montevecchi FM. Possible role of decorin glycosaminoglycans in fibril to fibril force transfer in relative mature tendons–a computational study from molecular to microstructural level. *J Biomech.* 2003;36(10):1555-1569.
26. Kyriakides TR, Zhu YH, Yang Z, Bornstein P. The distribution of the matricellular protein thrombospondin 2 in tissues of embryonic and adult mice. *J Histochem Cytochem.* 1998;46(9):1007-1015.
27. Szántó T, Joutsi-Korhonen L, Deckmyn H, Lassila R. New insights into von Willebrand disease and platelet function. *Semin Thromb Hemost.* 2012;38(1):55-63.
28. Qiu Y, Brown AC, Myers DR, et al. Platelet mechanosensing of substrate stiffness during clot formation mediates adhesion, spreading, and activation. *Proc Natl Acad Sci USA.* 2014;111(40):14430-14435.
29. Kee MF, Myers DR, Sakurai Y, Lam WA, Qiu Y. Platelet mechanosensing of collagen matrices. *PLoS One.* 2015;10(4):e0126624.
30. Pimanda JE, Annis DS, Raftery M, Mosher DF, Chesterman CN, Hogg PJ. The von Willebrand factor-reducing activity of thrombospondin-1 is located in the calcium-binding/C-terminal sequence and requires a free thiol at position 974. *Blood.* 2002;100(8):2832-2838.